Analysis of the Mechanism of Lysozyme Pressure Denaturation from Raman Spectroscopy Investigations, and Comparison with Thermal Denaturation

ARTICLE *in* THE JOURNAL OF PHYSICAL CHEMISTRY B · MAY 2011

Impact Factor: 3.3 · DOI: 10.1021/jp2014836 · Source: PubMed

3 AUTHORS, INCLUDING:

Alain Hédoux
Université des Sciences et Technologies de L…
94 PUBLICATIONS **1,243** CITATIONS
SEE PROFILE

Yannick Guinet
Université des Sciences et Technologies de L…
86 PUBLICATIONS **1,178** CITATIONS
SEE PROFILE

THE JOURNAL OF PHYSICAL CHEMISTRY B

ARTICLE

pubs.acs.org/JPCB

Analysis of the Mechanism of Lysozyme Pressure Denaturation from Raman Spectroscopy Investigations, and Comparison with Thermal Denaturation

Alain Hédoux,* Yannick Guinet, and Laurent Paccou

Univ Lille Nord de France, F-59000 Lille, France; USTL, UMET, CNRS UMR 8207, F-59650 Villeneuve d'Ascq, France

ABSTRACT: Pressure denaturation of lysozyme dissolved in H_2O and D_2O was analyzed using Raman investigations in a wide frequency range. The simultaneous analysis of regions corresponding to the molecular fingerprint of the protein (500−1800 cm^{-1}), and the low- (50−450 cm^{-1}) and high- (2600−3800 cm^{-1}) frequency spectra, allow us to probe protein denaturation and the organization of water molecules. The pressure- and heat-induced transformations are compared. Both pressure- and heat-denatured states are obtained through an intermediate state characterized by intact secondary structure and enhanced water penetration in the tertiary structure. As a consequence of a weaker penetration upon pressurizing, it was found that the pressure-denatured state was partially unfolded compared with the heat-denatured state. The mechanism of pressure denaturation was related to the disruption of the hydrogen-bond network of water onto a set of clusters characterized by strengthened O − H interactions, inducing a hardening of protein dynamics. The mechanism is opposite to that observed upon heating, i.e., the softening of the hydrogen bond network of water inducing a softer protein dynamics. The analysis of the intramolecular O−H stretching reveals that pressurizing lysozyme aqueous solution favors the development of low-density water from the protein surface to the bulk, contrasting to the compression of pure water leading to crystallization of high-density ice-VI.

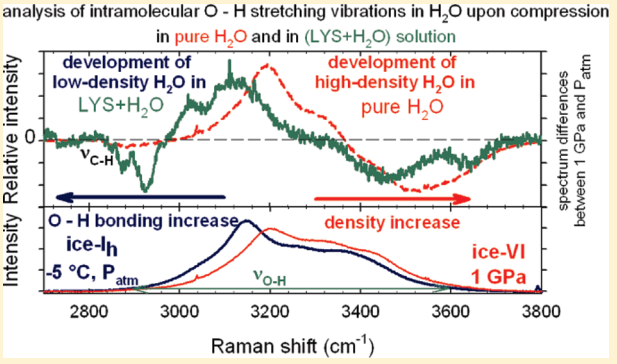

1. INTRODUCTION

It is well-known that proteins are thermodynamically stable only in a defined temperature interval, limited by two temperatures at which cooperative transitions lead to the loss of the protein activity or to a change of its function. At high temperatures, protein thermal unfolding has been widely investigated, and the mechanism of thermal denaturation was currently described for model proteins,[1−10] mainly from spectroscopic and calorimetric investigations. On the contrary cold-induced denaturation is much less studied, probably because it occurs below the freezing point of water. However, cold-induced denaturation is recognized as the most widespread environmental stress on many forms of life,[11] and also involved in lyophilization technologies currently used for the storage of foods and therapeutic materials.[12] Several strategies can be used to analyze the molecular mechanisms of protein cold-induced denaturation. The freezing point of the aqueous solution can be depressed by the addition of cosolvents to bring it below the temperature of cold denaturation. The addition of denaturants such as urea[12] or guanidine hydrochloride depressed the freezing point of the aqueous solution and also induces the increase of cold denaturation temperature. However, these cosolvents partially denature the native state of the proteins, and therefore the origin of the cold denaturation cannot be fully analyzed. Cryosolvents such as methanol or glycerol are well-known to lower the freezing temperature of the solvent, but also to stabilize the native state of proteins.[11] Alternatively, protein can be denatured by increasing the pressure at very high values (>500 MPa) in absence of ice,[13−16] indicating that pressure can be used as a destabilizer of structure and as antifreeze, without chemical modification of the solvent. It is now well recognized that the protein stability is characterized by an ellipsoidal (P,T)-phase diagram.[13,17−19] This description is based on the assumption that there exist only two states, the native − and the denatured − states of the protein. This suggests that all the denatured protein structures are of the same kind. From calorimetric data, the unfolded states were found to be similar[20] after the cold and heat denaturation, whereas more detailed spectroscopic studies did not support this description. Previous studies have pointed out that conformationally and mechanistically, the pressure and cold unfolding processes are found to be very alike, while the heat unfolding shows some pronounced differences.[21,22] Structural differences have also been found between the cold- and heat-denatured states of β-lactoglobulin.[23] Despite that, controversial considerations are reported on similarities between cold, pressure, and heat induced structural changes,[20−23] pressure appears as an interesting way to analyze the

Received: February 15, 2011
Revised: April 12, 2011
Published: May 04, 2011

dx.doi.org/10.1021/jp2014836 | J. Phys. Chem. B 2011, 115, 6740–6748

mechanism of cold denaturation, since no cosolvent must be used to reach the denatured state.

Spectroscopic techniques are suitable for analysis of the secondary structure from the investigation of amide modes[5,24] and then for monitoring the unfolding process of the secondary structure.[1,10] However, most of previous spectroscopy studies carried out to investigate the pressure denaturation[14−16,25,26] have been focused only on the vibrational bands of the protein, and then give the structural description of the denatured state, without direct information on the mechanism of denaturation. Raman investigations on protein thermal denaturation,[1,10] simultaneously performed in the amide I region and in the low-frequency (10−350 cm^{-1}) have given a clear description of the mechanism of thermal denaturation through the analysis of the solvent dynamics and its coupling with that of the protein.

In the present work, we use the same methodology to analyze the mechanism of pressure-induced denaturation of lysozyme to obtain information on the origin of the pressure denaturation. Lysozyme (LYS) is a globular protein (16 kDa) with a secondary structure mainly composed of α-helices (∼40−45%) and also containing β-sheet structures (∼20%).[5,24,27] Raman investigations were carried out in the (500−1800 cm^{-1}) region for monitoring the secondary structure of the protein through the analysis of amide I and III modes and to analyze the vibrations of the side chains, in the OH-stretching region (2600−3800 cm^{-1}) to probe structural changes in the hydrogen bond network of water, and in the low-frequency range (50−450 cm^{-1}) to analyze the dynamics of the solvent, the protein, and the coupling between them.

2. MATERIALS AND METHODS

Lysozyme was purchased from Sigma as lyophilized powder (purity minimum 90%). Lysozyme solutions were prepared by dissolving lysozyme in H_2O and in D_2O (10 wt %). Raman spectra were recorded with Renishaw's *InVia* Raman microscope, comprising a single-grating spectrograph coupled to an optical microscope, and using ∼150 mW of 785 nm line of a Renishaw diode for excitation. A Renishaw setting of four high-performance filters leads to the rejection of the scattered light below 50 cm^{-1}.

Pressure was generated in a gasketed membrane diamond-anvil cell (MDAC). Three ruby crystals (size ∼10 μm) were included for in situ pressure measurements by the standard ruby fluorescence technique.[28] The whole Raman spectrum (50 − 3800 cm^{-1}) of lysozyme dissolved in H_2O was recorded upon compression from 20 MPa up to 900 MPa, while only amide I band was analyzed upon compression and decompression. For lysozyme dissolved in D_2O, only the amide I mode was analyzed upon compression. Pressurization of H_2O was also investigated in the intramolecular O−H stretching region between 2800 and 3800 cm^{-1}.

High-temperature data on lysozyme dissolved in H_2O and D_2O were obtained from previous investigations.[1]

3. RESULTS

3.1. Fingerprint Region. The spectrum of the molecular fingerprint of LYS, lying on the 500−1800 cm^{-1} frequency range was decomposed in two regions.

3.1.1. Analysis of the Amide I Mode. The 1500−1800 cm^{-1} region is dominated by the amide I band, which can be used for the determination of the secondary structure,[24] and then for monitoring the unfolding process of the secondary structure. This band arises mainly from the C═O stretching vibration with minor contributions of the C—N stretching vibration, and the

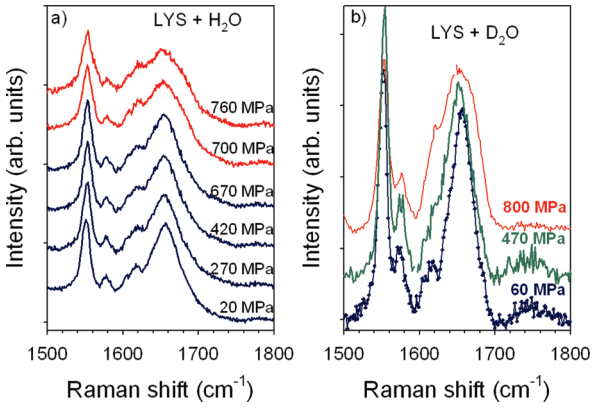

Figure 1. Pressure dependence of the Raman spectrum in the amide I region, (a) for LYS dissolved in H_2O, (b) for LYS dissolved in D_2O.

N—H in-plane bend. This latter is responsible for the sensitivity of the amide I band to NH/ND exchanges in the protein backbone.[29] In this context, a frequency downshift of amide I band was connected to enhanced isotopic exchanges associated with the solvent penetration in a more flexible tertiary structure during thermal denaturation of globular proteins.[1,10] Consequently, dissolving proteins in D_2O gives the opportunity to detect the transformation of the tertiary structure, while amide I mode in proteins dissolved in H_2O gives only information on conformational changes in the protein backbone. The pressure dependences of the amide I band are plotted in Figure 1a,b for LYS dissolved in H_2O and D_2O, respectively. Both figures show frequency downshifts of amide I band upon pressurization, prior to a shift toward the high frequencies associated with a broadening of the band, recognized as the signature of the unfolding process of the secondary structure upon heating[1] and pressurizing.[14,16] The band shape of the amide I mode was fitted using a mixed contribution of Lorentzian and Gaussian shapes, and the pressure behavior of the frequency of the amide I band is reported in Figure 2a for lysozyme dissolved in H_2O and in Figure 2b for lysozyme dissolved in D_2O. It is clearly observed that the frequency downshift is more marked for lysozyme dissolved in D_2O. This frequency downshift is probably resulting from two effects. (i) The decrease of the interatomic O···H distances by compression that favors hydrogen bonding in α-helix and β-sheet structures, and then is observed for LYS dissolved in H_2O and D_2O. (ii) The second effect, only observed in D_2O, corresponds to the enhancement of the NH/ND exchanges induced by the solvent penetration in the protein interior as observed upon heating.[1] This could be the indication that pressure unfolding could occur via a "molten globule state" as previously suggested,[16] in a process similar to that of the thermal denaturation.[1] Consequently, the frequency downshift observed for LYS dissolved in H_2O can be considered as the consequence of the compression of α-helices, and the frequency downshift of the amide I band should not be considered as the signature of pressure unfolding, as previously reported from infrared spectroscopy measurements on human serum albumin[15] (HSA) and lysozyme[14,16] dissolved in D_2O. An upshift in the frequency of amide I band is clearly observed in Figure 2a upon depressurization from the denatured state, probably inherent to the depressurization effect of the protein backbone. Upon further depressurization below 600 MPa, a downshift of the frequency is clearly observed reflecting refolding process, at pressure significantly lower than the pressure of

dx.doi.org/10.1021/jp2014836 |J. Phys. Chem. B 2011, 115, 6740–6748

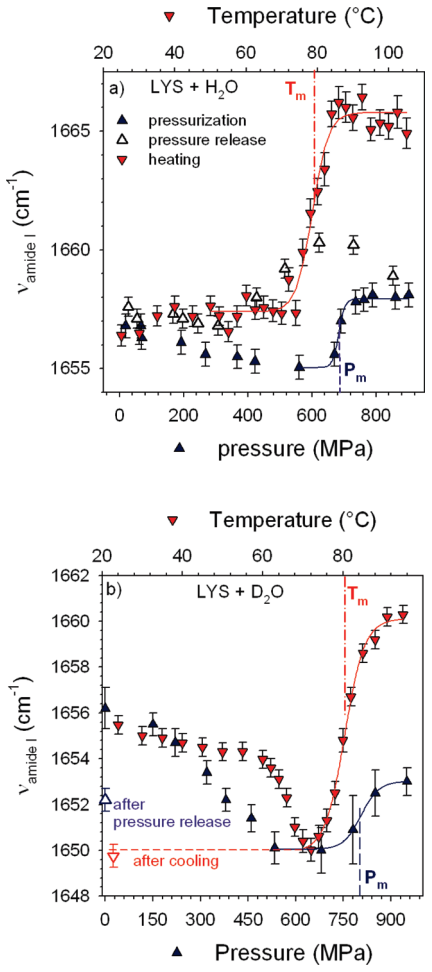

Figure 2. Pressure and temperature dependences of the frequency of the amide I band, (a) for LYS dissolved in H_2O upon pressurizing and depressurizing, (b) for LYS dissolved in D_2O upon pressurizing. Open up and down triangles corresponds to the frequency of amide I band after pressure release and cooling at ambient conditions.

unfolding. Similar frequencies determined near P_{atm} before and after denaturation indicate the reversibility of pressure-induced transformation of LYS. The pressure dependence of the frequency of amide I band was fitted using a sigmoid-shaped curve, $\nu = [(\nu_N - \nu_D)/(1 + (\exp(P - P_m)/\Delta P))] + \nu_D$, similar to that previously used to describe LYS thermal unfolding,[1,30] where ν_N and ν_D represent amide I frequency in the native and denatured states, P_m the midpoint pressure and ΔP the half interval of denaturation. This fitting procedure gives the midpoint pressure denaturation P_m, and $\Delta\nu = (\nu_D - \nu_N)$ representative of the degree of denaturation,[31] reported in Table 1 for LYS dissolved in H_2O and D_2O. The analysis of Table 1 and Figure 2a,b clearly reveals a higher denaturation pressure of LYS in D_2O with a midpoint pressure estimated at about $P_m \approx 800$ MPa, compared to that determined in presence of H_2O ($P_m \approx 690$ MPa), but a similar degree of denaturation with $\Delta\nu \approx 3$ cm^{-1}.

3.1.2. Analysis of 500−1200 cm^{-1} Region. The 500−1200 cm^{-1} spectrum reported in Figure 3 is mainly composed of Raman bands reflecting vibrations of aromatic side chains.

The Raman band near 875 cm^{-1} was assigned to the vibrational mode W17 of Tryptophan residues(Trp), recognized as an indicator of H-bond strength.[32] The frequency of the W17 band

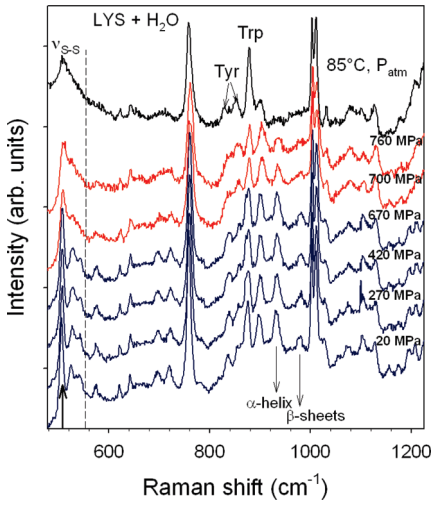

Figure 3. Pressure dependence of the Raman spectrum LYS dissolved in H_2O in the 500−1200 cm^{-1} region. The spectrum in the pressure-denatured state at 760 MPa is compared to that of heat-treated sample at 85 °C. Arrows localize Raman bands analyzed in the present work.

Table 1. Fitted Parameters of Denaturation Curves Plotted in Figure 2a,b, for Pressure and Temperature Denaturations of Lysozyme Dissolved in H_2O and D_2O

	P_m (MPa)	$\Delta\nu(P)$ (cm^{-1})	T_m (°C)	$\Delta\nu(T)$ (cm^{-1})
LYS + H_2O	686 ± 2	2.9 ± 0.2	78.6 ± 0.2	8.4 ± 0.5
LYS + D_2O	806 ± 5	3.0 ± 0.2	80.4 ± 0.2	10.1 ± 0.5

was determined by a fitting procedure and plotted against pressure in Figure 4a. An upshift in the frequency from 874 cm^{-1} in the native state toward 880 cm^{-1} in the denatured state is clearly observed, indicating a weakening of H-bond strength. This frequency shift most likely results from increased flexibility of the Trp side chain and transient associations with water molecules, yielding weaker H-bonds.

For proteins containing Tyrosyl (Tyr) residues, it is recognized that the intensity ratio of the doublet near 850 and 830 cm^{-1} is sensitive to the nature of the hydrogen bonding of the phenolic hydroxyl group,[33] depending on the environments of the tyrosyl side chains. This intensity ratio was determined from a fitting procedure and plotted against pressure in Figure 4b. The value obtained in ambient conditions is consistent with previous Raman investigations[34] and suggests that Tyr residues are mainly located on the protein surface. The intensity increase of the higher frequency component of the doublet is commonly observed through protein denaturation.[33] This change can be interpreted as induced by different environments of Tyr side chains upon pressurizing, as previously observed by thermal stress[35] or by the disruption of the strong hydrogen bonds of Tyr residues.[33]

The 500−550 cm^{-1} region was assigned to stretching vibrations of disulfide bridges.[36] At ambient pressure, three Raman bands are clearly detected at 505, 525, and 540 cm^{-1} corresponding to three different conformations of disulfide bonds, also observed in other Raman investigations.[35] It is clearly observed in Figure 3 that the 540 cm^{-1} component disappears at 700 MPa, and becomes a tail on the high frequency side of the 525 cm^{-1} component. Upon further pressurization, this latter is detected as a broad and pronounced shoulder of the 505 cm^{-1} band. The pressure

dx.doi.org/10.1021/jp2014836 |J. Phys. Chem. B 2011, 115, 6740–6748

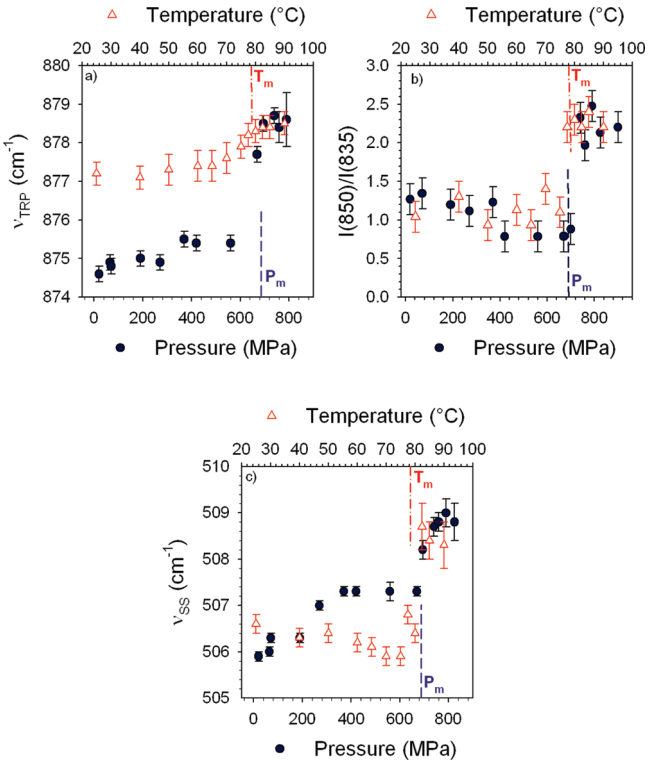

Figure 4. Pressure and temperature dependences of Raman mode parameters associated with side-chain vibrations: (a) frequency of vibrations of tryptophan (Trp) residues; (b) intensity ratio of the doublet located around 850 and 830 cm^{-1}, corresponding to vibrations of tyrosyl (Tyr) residues; (c) frequency of stretching vibrations of disulfide bridges. P_m and T_m reported on these plots correspond to midpoint pressure and temperature determined from the fit of the pressure and dependences of the amide I frequency.

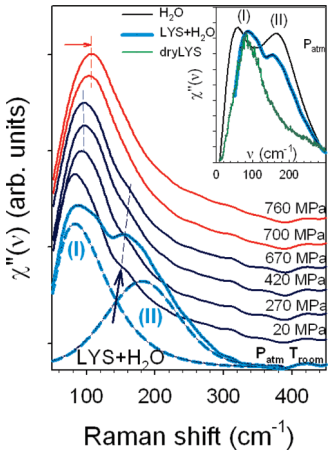

Figure 5. Pressure dependence of the low-frequency Raman spectrum in the 50−450 cm^{-1} region of LYS dissolved in H_2O; the low-frequency spectra of dry LYS, H_2O and LYS dissolved in H_2O are plotted in the inset. The log-normal and Gaussian components, corresponding to bands (I) and (II), respectively, determined from the fitting procedure of the low-frequency spectrum at atmospheric pressure and room temperature, are plotted in dashed line. Band (I) mainly reflects protein dynamics and solvent−protein interactions and band (II) corresponds to intermolecular O—H stretching vibrations in the H-bond network of water. The horizontal red arrow indicates the upshift of band (I) above 670 MPa, while the blue arrow and associated dashed line shows the disappearance of band (II) upon pressurization.

dependence of the most intense band located at 505 cm^{-1} is plotted in Figure 4c. This plot clearly shows an upshift of the frequency upon pressurization from atmospheric pressure up to 600 MPa, and a sudden frequency shift above 670 MPa, accompanying modifications of the Raman band shape around 525 and 540 cm^{-1}. The analysis of disulfide vibrations reveals a strong distortion of disulfide bonds accompanying the unfolding process. The spectrum at 760 MPa in the denatured state indicates that the disulfide bonds in lysozyme are predominant in a slightly distorted gauche−gauche−gauche conformation.[36]

The Raman bands located at 930 and 960 cm^{-1} were assigned to Cα−C−N stretching vibrations[35] in α-helices and β-sheets, respectively, and then can be used to determine the content of α-helix and β-sheet structures in the secondary structure. The intensity of the 930 cm^{-1} band related to the α-helix structures suddenly decrease at 700 MPa, indicating a loss of α-helices. The intensity at 800 MPa is estimated to about 46% of that determined in the native state. In contrast, the 960 cm^{-1} band broadens above 700 MPa, and gives distinguishable intensity to the spectrum plotted in Figure 3, not easily estimated because of its broadening.

3.2. Analysis of the Low-Frequency Range (50−450 cm^{-1}). The low-frequency spectrum of proteins in solution gives information on the dynamics of the protein, the solvent and their coupling.[1,10,37] The Raman intensity is converted into Raman susceptibility $\chi''(\nu)$, according to a procedure previously described,[1,10,37,38] which is generally considered as representative of the vibrational density of states in molecular disordered systems. The pressure dependence of the $\chi''(\nu)$-spectrum for LYS dissolved in water is plotted in Figure 5. The Raman susceptibility of water (W) is compared to those of dry LYS and LYS dissolved in water in the inset of Figure 5. This comparison gives a clear assignment of both broad bands detected in the spectrum of LYS in solution. The low-frequency band (I) located at 80 cm^{-1} mainly reflects the dynamics of LYS, and the solvent−protein interactions,[38] while the band (II) at 180 cm^{-1} is assigned to intermolecular O—H stretching vibrations in the H-bond network of water. Band (II) is then associated with the collective dynamics of the H-bond network of water,[38] giving direct information on the structural organization of water molecules. Inset of Figure 5 shows that the intensity of band II is significantly lower in the spectrum of lysozyme aqueous solution than in water. The reduction in intensity of band (II) corresponding to collective vibrational modes of the H-bond network of water shows that H-bonded structure of water molecules extends over a weaker range in presence of lysozyme. The frequencies of both Raman bands were determined from a fitting procedure using a log-normal function and a Gaussian to describe the shape of the bands I and II, respectively. Both fitted bands resulting from the fitting procedure by the residue method of the PEAKFIT peak analysis software (Jandel Scientific) are plotted in thick dashed lines in Figure 5 for hydrated LYS under ambient conditions. The pressure dependences of these frequencies are reported in Figure 6. Upon low compression, the intensity of the $\nu_{OH\cdots O}$ band (II) (see blue arrow in Figure 5) significantly decreases. Upon further compression, band (II) becomes a shoulder of the band (I) (dashed blue line) which is not distinguishable above 670 MPa in Figure 5. Figure 6 indicates that band II significantly shifts toward the high frequencies. Consequently, the observed effect on the H-bond network of water by adding lysozyme is amplified upon pressurizing. The disruption of the H-bond network leads to a set of clusters, characterized by strengthened O—H interactions. At 700 MPa, the $\chi''(\nu)$-spectrum

dx.doi.org/10.1021/jp2014836 |J. Phys. Chem. B 2011, 115, 6740–6748

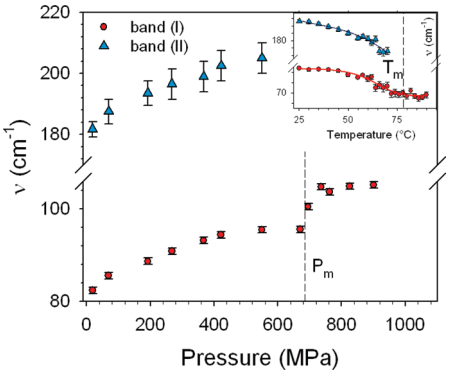

Figure 6. Pressure dependence of the frequency of the low-frequency bands in the spectrum of LYS dissolved in H_2O, obtained from a fitting procedure described in the text. The temperature dependences of the same bands are reported in the inset. P_m and T_m are determined from the pressure and temperature dependences of the amide I frequency.

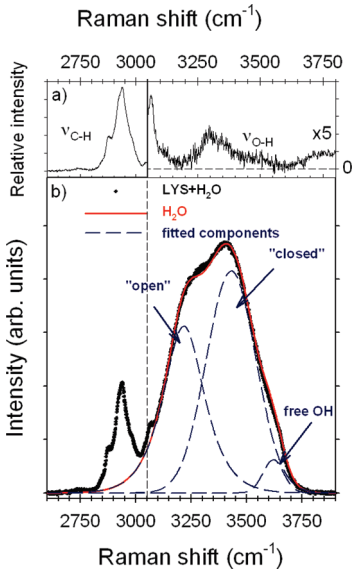

Figure 7. Comparison of the intramolecular O—H stretching spectra of H_2O and LYS dissolved in H_2O: (a) spectrum difference between (LYS + H_2O) and H_2O; and (b) Raman intensity of (LYS + H_2O) and H_2O.

is dominated by a broad band around 105 cm^{-1}, and the contribution of the band (II) was suppressed in the fitting procedure. Above 670 MPa, a jump of band (I) toward the high frequencies is clearly observed in Figures 5 (see horizontal red arrow) and 6. Under similar pressures, the unfolding of the secondary structure is observed in Figure 2a, through the frequency shift of the amide I band, indicating a close relation between conformational changes and the protein dynamics, probably inherent to the distortion of the H-bond network of water.

3.3. Analysis of the High-Frequency Region (2600−3800 cm^{-1}). The intramolecular O—H stretching vibrations (2600−3800 cm^{-1} region), which overlaps with the minor contribution of intramolecular C—H stretching vibrations in LYS is very sensitive to the local H-bonding structure. The spectra of LYS dissolved in H_2O (LW) and water (W) are plotted in Figure 7 under room conditions. The spectrum can be fitted using only 3 Gaussian components represented with dashed lines in Figure 7.

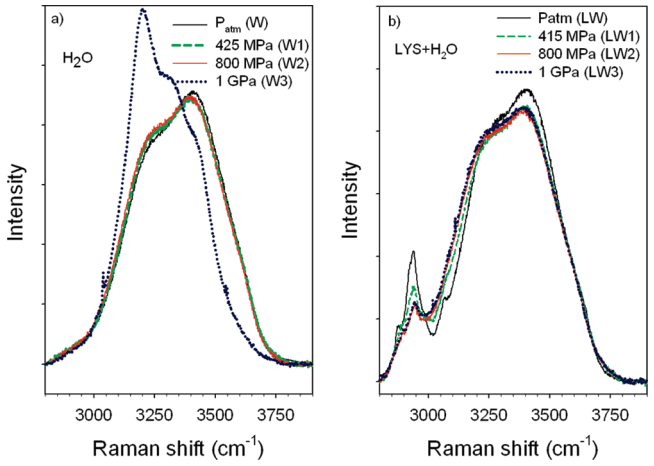

Figure 8. Pressure dependence of the intramolecular O—H stretching spectrum (a) For H_2O and (b) For LYS dissolved in H_2O.

In this context, these bands can be attributed[39] to (i) the O—H stretch in the tetrabonded water molecules, named "open" component corresponding to the band dectected at 3250 cm^{-1}, (ii) the same vibration in the distorted H-bond network ("closed" component at 3450 cm^{-1}), and (iii) O—H stretching vibrations in free water molecules at 3605 cm^{-1}. In other studies, four components are used in the fitting procedure[40,41] with different interpretations. However, it is commonly recognized that an increase of the strength of the hydrogen bond induces a frequency downshift of intramolecular OH stretching vibrations. The (LW-W) spectrum difference plotted in figure 7, shows that addition of LYS in water induces very weak changes in the ν_{O-H} spectrum of water, and then has only a very weak influence on the H-bond network of water, except around the protein surface. The enhanced intensity observed in the (LW-W) spectrum difference and in the LW spectrum around 3300 cm^{-1} in Figure 7a,b, corresponds to intramolecular O—H stretching in LYS or/and additional H-bonding between water and protein with intermediate strength. The pressure dependences of the ν_{O-H} spectra in water and LYS aqueous solution are plotted in Figure 8a,b, respectively. In both cases, the intensity increase of the "open" component is clearly observed, with a concomitant decrease of the intensity of the "closed" component upon pressurizing. These changes are more marked in the presence of LYS between atmospheric pressure and 800 MPa. This unequivocally shows an increase of the strength of hydrogen bonds upon pressurizing. Figure 8 shows that the solvent transforms into the crystallized ice-VI upon further pressurizing up to about 1 GPa, in agreement with previous studies.[42] The spectrum of ice-VI is dominated by an intense band around 3200 cm^{-1}, as observed in the Raman spectrum of the High Density Amorphous (HDA) state of ice.[43] This band is observed to be upshifted about 100 cm^{-1} above the position of the most intense band of the hexagonal ice-I_h spectrum,[44] reflecting a higher density and weaker H-bonding. A more detailed description of the local hydrogen-bonding structure in H_2O in the absence and presence of lysozyme can be obtained from the ν_{O-H}-spectral differences between atmospheric and high pressure states plotted in Figure 9a. The spectra of ice-I_h and ice-VI are plotted in Figure 9b,c to directly analyze the relationship between the features emerging from pressurization of water and LYS solution as a function of spectral signatures of ice-I_h and ice-VI. The (LW1-LW) and (LW3-LW) spectrum differences indicate the emergence of a double hump in

dx.doi.org/10.1021/jp2014836 |J. Phys. Chem. B 2011, 115, 6740–6748

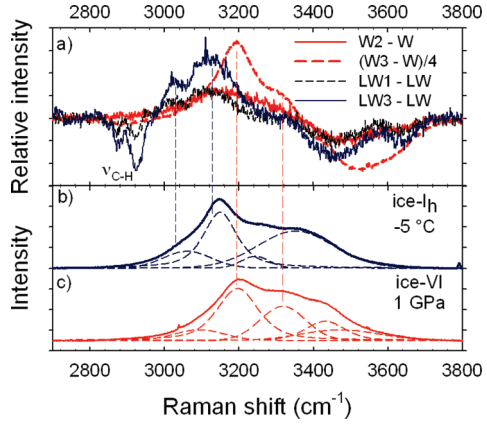

Figure 9. Influence of pressure on the O—H stretching spectrum; comparison between the following: (a) Spectrum differences between pressurized states (415, 1000 MPa) and ambient conditions of LYS aqueous solution, and between pressurized states (800, 1000 MPa) and ambient conditions of water. The relative intensity of the (W3−W) spectrum difference is divided by 4 for clarity reasons; (b) Spectrum of ice-I_h recorded at −5 °C; and (c) Spectrum of ice-VI recorded at room temperature and about 1 GPa.

the 2950−3250 cm^{-1} range upon pressurizing, corresponding to both low-frequency bands of ice-I_h (see vertical blue dashed lines in Figure 9), while the spectrum differences in H_2O show the development of the predominant Raman bands of ice-VI around 3200 cm^{-1}. The features observed in the spectrum differences of LYS aqueous solution, are too large to be only attributed to specific pressure behavior of the hydration water. However, Figure 9 shows that the organization of the water molecules is widely influenced, upon pressurizing, by the protein in an extent probably depending on its size,[20,45,46] while under atmospheric pressure, the influence of LYS on the local order of water molecules is hardly detectable in Figure 7. The region of the frequency where the emerging intensity is detected in Figure 9a (2900−3250 cm^{-1}) indicates the development of the low-density tetrahedral structure of ice-I_h, probably from the hydration shells into the bulk water, since high-density ice-VI develops upon compression in the absence of LYS (see the intensity increase around 3200 cm^{-1} in Figure 9).

The fitting procedure of the ν_{O-H} spectrum for the lysozyme solution and H_2O gives the pressure dependence of the low frequency component for water in presence and in absence of lysozyme plotted in Figure 10. The intensity increase observed in Figure 9a in the 2950−3250 cm^{-1} is associated with the frequency downshift of the ν_{O-H} band. The downshift is more marked in the P_{atm} − 800 MPa range in presence of lysozyme, because the intensity increase is observed at lower frequencies. It can be noticed that the frequency of the "open" component in water is nearly pressure independent upon pressurizing to about 600 MPa. Above 600 MPa, the component significantly shifts toward lower frequencies, i.e., the position of the band in ice-VI, reflecting an increase in the hydrogen bond strength[44] associated to the increase of density. By contrast to water, the same component in the lysozyme solution has clear linear pressure dependence up to 800 MPa. Above 800 MPa, i.e., in the pressure denatured state of LYS, the H-bond network of water becomes pressure independent. The discrepancies observed in Figures 8, 9, and 10, between O—H stretching vibrations in LYS aqueous solution and water reflect the considerable influence of LYS on the pressure behavior of the H-bond network of water.

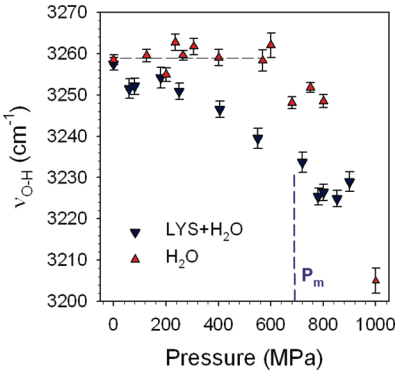

Figure 10. Pressure dependence of the frequency of the "open" component of O—H stretching vibrations in H_2O and LYS dissolved in H_2O. P_m is the midpoint pressure determined from the pressure dependence of the amide I frequency.

4. DISCUSSION

4.1. Comparison between Pressure and Thermal Denatured States. It is well recognized that pressurization of molecular compounds induces frequency shifts of intramolecular vibrational modes[47,48] with negative $(\partial\nu/\partial P)$ for X—H bonds involved in H-bonding. Consequently, pressurization induces a significant frequency downshift of the amide I mode, while the secondary structure remains intact. To discriminate frequency shifts induced by conformational changes from those induced by compression of atomic bonds, we used the frequency difference $(\Delta\nu = \nu_D - \nu_N)$ of amide I band, which has been recently connected to the loss of protein activity.[31] Table 1 indicates similar $\Delta\nu$-values in the pressure denatured state of LYS dissolved in H_2O and D_2O, which are drastically different from those determined upon heating LYS solutions. This clearly reveals that a large content of the secondary structure remains in the folded conformation after denaturation at high pressure, as previously reported for other proteins.[21,22,49] Additional information can be obtained from the comparison of the amide I frequency under ambient conditions after denaturation by compression and by heating of LYS dissolved in D_2O. Assuming reversibility of the denaturation process upon heating from previous investigations[1] and pressurizing from the present study (see Figure 2a), the frequency of amide I band plotted in Figure 2b under ambient conditions clearly indicates that (i) solvent penetration is detected upon pressurizing, and (ii) the enhancement of isotopic exchanges is more important when the sample is heated, since the frequency of the amide I mode is lower after cooling than after decompression. This observation suggests a deeper penetration of water in the protein interior during heating than during compression, and thus a minor exposition of hydrophobic residues to the solvent at high pressure compared to high temperature. Figure 3 clearly shows that the 930 cm^{-1} Raman band corresponding to vibrations in α-helices is more intense at 760 MPa than at 85 °C, for LYS dissolved in H_2O. In the thermal denatured state, the integrated intensity is determined to be about 10% of that measured at ambient conditions, instead of 46% in the pressure denatured state. This indicates that about twice more α-helix structures are unfolded in the heat-treated sample compared with the pressure denatured state. The 960 cm^{-1} band associated with β-sheets is clearly more broadened at 85 °C than at 760 MPa, reflecting a higher degree of disorder at high temperature. Figure 4a−c

dx.doi.org/10.1021/jp2014836 |J. Phys. Chem. B 2011, 115, 6740–6748

shows similar features in pressure and heat denatured states of various side chains (Trp, Tyr, disulfide bridges) reflecting similar denaturation around the protein surface. A significant content of secondary structure remains intact upon pressurization, probably because of a lower water penetration within lysozyme. This result is in line with the description of pressure unfolded proteins from different kinds of experiments, as relatively compact water-swollen structures with residual secondary structure,[49,50] and the determination of the high compactness of the pressure-denatured state.[51,52] Small Angle X-ray Scattering (SAXS) measurements on T4 LYS mutants[52] are also consistent with water penetration of the protein as the mechanism of pressure denaturation. SAXS is generally used to probe the pressure dependence of the tertiary and quaternary structures[53] via the analysis of the shape and the size of structural entities. Raman spectroscopy provides complementary specific and quantitative information on unfolding structures in pressure- and heat-treated samples at the molecular level, via intensity changes, broadening and frequency shifts of internal modes in the fingerprint region of lysozyme. In this region, isolated bands corresponding to well identified internal vibrations (stretching of disulfide bridges, Tyr and Trp vibrations, amide I, II and III modes), are very sensitive to the molecular conformation and the molecular organization surrounding the atomic bonds both in the protein backbone and around side-chains residues. The description of the pressure denatured state given in the present work in terms of more compact molten globule and denatured states, is in agreement with SAXS measurements on different proteins.[49,52] No additional conformational changes were detected at pressures above 800 MPa, as previously reported,[54] suggesting plurality of pressure-denatured forms in lysozyme. The two-step changes upon pressurizing detected from the ultraviolet fluorescence of LYS[54] could correspond to the penetration of the solvent in the protein prior the unfolding process, which is observed as complete around 800 MPa in the present work.

4.2. Mechanism of Pressure Denaturation. It is known that pressure denaturation is associated with a negative volume change.[55−57] The volume change, ΔV, for pressure denaturation of LYS, can be calculated from the relation[56] $(\partial \ln K_{eq})/\partial P = V/RT$, where T is the temperature, R is the gas constant, and K_{eq} is the equilibrium constant of the two state-denaturation. It can be calculated from[1] $K_{eq} = (\nu_N - \nu)/(\nu - \nu_D)$, ν_N and ν_D corresponding to the frequencies of amide I mode in the native and denatured states. The volume change was calculated for LYS dissolved in D_2O and H_2O. A volume change of about −90 (±20) ml/mol was obtained at 800 MPa for LYS dissolved in D_2O, in agreement with the estimation of ΔV between −50 and −100 mL/mol reported by Li et al.[54] However, a value of −245 (±50) ml/mol was determined around P_m = 686 MPa in LYS dissolved in H_2O. This difference between these two values of ΔV is not necessarily related to the nature of the solvent, but probably to the lack of experimental data around P_m.

The description of protein−water interactions is fundamental for the prediction of protein physical properties,[58] and protein stabilization is recognized to be intimately related to hydration water.[11,59] Table 1 clearly indicates higher temperature and pressure of denaturation in D_2O than in H_2O. The stabilizing effect of D_2O, widely observed for protein thermal denaturation,[1,10,60−62] was mainly interpreted as resulting from an increase of the protein rigidity[61] in presence of D_2O. This effect was determined to be more marked at higher temperature[61] probably because of the temperature dependence of the hydrogen-bond network in D_2O.[1,10] In opposition to heating, the pressure behavior of the hydrogen-bond network in D_2O could maintain the protein flexibility upon compression. The present Raman study gives the opportunity to simultaneously analyze the pressure behavior of the H-bond network of water and the pressure-induced transformation of LYS. It is well-known that water influences protein dynamics with signatures detected in the very low-frequency region (<50 cm^{-1}) by inelastic neutron scattering,[63] not accessible with the spectrometer configuration. However, present investigations reveal that LYS does not induce significant modification of the local H-bonded structure in bulk water at atmospheric pressure while drastic differences can be observed on water dynamics in hydration shells and bulk water from neutron quasi-elastic scattering.[64] By contrast, LYS has a drastic influence on the organization of water molecules upon pressurizing. Figure 9 clearly reveals the strengthening of the hydrogen bonds between water molecules, in agreement with the pressure dependence of band (II) in the low-frequency range. In presence of LYS, the tetrahedral structure of ice-I_h develops upon pressurizing, while in the absence of LYS the emerging Raman intensity between atmospheric and high pressure states, is distinctive of the high-density ice-VI crystalline phase. This result is in line with molecular dynamics simulations,[58,65] which show that the hydration shell compressibilities near protein surface decrease with increasing attraction. In this context, the development of ice-I_h organization could be favored upon pressurizing rather than the denser ice-VI, around folded structure of LYS. However, Monte Carlo simulations[59] lead to a mechanism for cold denaturation at high pressure related to the loss of local low-density water structure. It is worth mentioning that the presence of low-density water organization around the protein surface is consistent with the weak water penetration into the protein, and the low degree of protein unfolding detected in the pressure-treated sample compared with that in the heat-treated sample.

Figure 6 shows that the development of the low-density water structure upon pressurizing is accompanied with a drastic hardening of protein dynamics. Pressure denaturation of LYS is associated with a discontinuous shift of band (I) toward the high frequencies, and no distinction can be observed between protein and water dynamics in the pressure denatured state. The inset of Figure 6 shows an opposite temperature behavior (upon heating)[1] of the protein and water dynamics, i.e., the softening of the H-bond network of water inducing a downshift of band (I) in the heat denatured state in which only one band was detected in the low-frequency range.

5. CONCLUSIONS

Raman investigations were carried out in a wide frequency range on LYS dissolved in H_2O and D_2O. Investigations in the fingerprint region (500−1800 cm^{-1}) of lysozyme gives information on the pressure denatured state with regard to the heat denatured state, while the analyzes of the low- and high-frequency ranges between 50−450 cm^{-1} and 2800−3800 cm^{-1} provide information on the organization of water molecules and then on the mechanism of pressure-induced transformation of lysozyme. It was found that pressurization favors the development of local low-density water structure similar to ice-I_h environment. In an opposite way to heat denaturation, the strengthening of intermolecular O−H interactions upon pressurizing, associated with structural modifications of H-bond network, imposes a considerable stiffening of protein dynamics. Another consequence is the weak water penetration into the protein, and then a low degree of unfolding in the

pressure-denatured state compared to that in the heat-denatured state. The rate of unfolded helices is about two times higher in the heat-treated samples. In contrast to the protein backbone, vibrational properties of side-chains are found to be similar in the heat- and pressure-denatured states. In both heat and pressure denaturations, the unfolding process of the secondary structure occurs from an intermediate state characterized by enhanced water penetration leading to a more flexible tertiary structure with intact secondary structure. Controversial results are reported in the literature concerning the comparison between heat- and pressure- or cold-induced protein transitions, considering similar[17,20,56] or different[23,49,54,66] transformation mechanisms and denatured states. The present work indicates a similar denaturation mechanism via an intermediate state (molten globule), probably more compact at high pressure than that obtained by heating, and a significantly low degree of unfolding in the pressure-denatured state with probably intact α-helix structures deeply buried in the tertiary structure. The two processes of denaturation at high pressure and temperature are closely related to the disruption of H-bonds in water structure leading to formation of clusters, which impose protein dynamics with inverse behaviors upon compression and heating.

AUTHOR INFORMATION

Corresponding Author

*Tel: +33 320434677; Fax: +33 320436857; E-mail:alain.hedoux@univ-lille1.fr.

ACKNOWLEDGMENT

This work was supported by the ANR (Agence Nationale de la Recherche) through the BIOSTAB project ("Physique Chimie du Vivant" program).

REFERENCES

(1) Hédoux, A.; Ionov, R.; Willart, J. F.; Lerbret, A.; Affouard, F.; Guinet, Y.; Descamps, M.; Prevost, D.; Paccou, L.; Danède, F. *J. Chem. Phys.* **2006**, *124*, 14703.
(2) de Wit, J.; Klarenbeek, G. *J. Dairy Res.* **1981**, *48*, 293.
(3) Bell, L. N.; Hageman, M. J.; Muraoka, L. M. *J. Pharm. Sci.* **1995**, *84*, 707.
(4) Baum, J.; Dobson, C. M.; Evans, P. A.; Hanley, C. *Biochemistry* **1989**, *28*, 7.
(5) Anderle, G.; Mendelsohn, R. *Biophys. J.* **1987**, *52*, 69.
(6) Griko, Y. V.; Privalov, P. L. *Biochemistry* **1992**, *31*, 8810.
(7) Ikeda, S.; Li-Chan, E. *Food Hydrocolloids* **2004**, *18*, 489.
(8) Nonaka, M.; Li-Chan, E.; Nakai, S. *J. Agric. Food Chem.* **1993**, *41*, 1176.
(9) Paulsson, M.; Hegg, P.-O.; Castberg, H. B. *Thermochim. Acta* **1985**, *95*, 435.
(10) Hedoux, A.; Willart, J. F.; Paccou, L.; Guinet, Y.; Affouard, F.; Lerbret, A.; Descamps, M. *J. Phys. Chem. B* **2009**, *113*, 6119.
(11) Franks, F.; Hatley, R. H. *Pure Appl. Chem.* **1991**, *63*, 1367.
(12) Tang, X. C.; Pikal, M. J. *Pharm. Res.* **2005**, *22*, 1167.
(13) Meersman, F.; Smeller, L.; Heremans, K. *Biochim. Biophys. Acta* **2006**, *1764*, 346.
(14) Heremans, K.; Wong, P. T. T. *Chem. Phys. Lett.* **1985**, *118*, 101.
(15) Smeller, L.; Meersman, F.; Heremans, K. *Eur Biophys J* **2008**, *37*, 1127.
(16) Smeller, L.; Meersman, F.; Heremans, K. *Biochim. Biophys. Acta* **2006**, *1764*, 497.
(17) Hawley, S. A. *Biochemistry* **1971**, *10*, 2436.
(18) Smeller, L. *Biochim. Biophys. Acta* **2002**, *1595*, 11.
(19) Kunugi, S.; Tanaka, N. *Biochim. Biophys. Acta* **2002**, *1595*, 329.
(20) Privalov, P. L. *Crit. Rev. Biochem. Mol.* **1990**, *25*, 281.
(21) Zhang, J.; Peng, X.; Jonas, A.; Jonas, J. *Biochemistry* **1995**, *34*, 8631.
(22) Meersman, F.; Smeller, L.; Heremans, K. *High Press. Res.* **2000**, *19*, 263.
(23) Griko, Y. V.; Kutyshenko, V. P. *Biophys. J.* **1994**, *67*, 356.
(24) Williams, R. W.; Dunker, A. K. *J. Mol. Biol.* **1981**, *152*, 783.
(25) Nash, D. P.; Jonas, J. *Biochemistry* **1997**, *36*, 14375.
(26) Nash, D. P.; Jonas, J. *Biochem. Biophys. Res. Commun.* **1997**, *238*, 289.
(27) Levitt, M.; Greer, J. *J. Mol. Biol.* **1977**, *114*, 181.
(28) Mao, H. K.; Xu, J.; Bell, P. M. *J. Geophys. Res.* **1986**, *91*, 4673.
(29) Surewicz, W. K.; Mantsch, H. H.; Chapman, D. *Biochemistry* **1993**, *32*, 389.
(30) Ionov, R.; Hédoux, A.; Guinet, Y.; Bordat, P.; Lerbret, A.; Affouard, F.; Prevost, D.; Descamps, M. *J. Non-Cryst. Solids* **2006**, *352*, 4430.
(31) Hédoux, A.; Krenzlin, S.; Paccou, L.; Guinet, Y.; Flament, M. P.; Siepmann, J. *Phys. Chem. Chem. Phys.* **2010**, *12*, 13189.
(32) Miura, T.; Takeuchi, H.; Harada, I. *Biochemistry* **1988**, *27*, 88.
(33) Siamwiza, M. N.; Lord, R. C.; Chen, M. C.; Takamatsu, T.; Harada, I.; Matsuura, H.; Shimanouchi, T. *Biochemistry* **1975**, *14*, 4870.
(34) Yu, N. T.; Jo, B. H. *Arch. Biochem. Biophys.* **1973**, *156*, 469.
(35) Zhao, W.; Yang, R. *J. Phys. Chem. B* **2010**, *114*, 503.
(36) Kudryavtsev, A. B.; Mirov, S. B.; DeLucas, L. J.; Nicolete, C.; van-der-Woerd, M.; Bray, T. L.; Basiev, T. T. *Acta Crystallogr. D* **1998**, *54*, 1216.
(37) Hédoux, A.; Willart, J. F.; Ionov, R.; Affouard, F.; Guinet, Y.; Paccou, L.; Lerbret, A.; Descamps, M. *J. Phys. Chem. B* **2006**, *110*, 22886.
(38) Lerbret, A.; Affouard, F.; Bordat, P.; Hédoux, A.; Guinet, Y.; Descamps, M. *J. Chem. Phys.* **2009**, *131*, 245103.
(39) D'Arrigo, G.; Maisano, G.; Mallamace, F.; Migliardo, P.; Wanderlingh, F. *J. Chem. Phys.* **1981**, *75*, 4264.
(40) Walrafen, G. E. *J. Chem. Phys.* **1967**, *47*, 114.
(41) Scherer, J. R.; Go, M. K.; Kint, S. *J. Phys. Chem.* **1974**, *78*, 1304.
(42) Walrafen, G. E. *J. Sol. Chem.* **1973**, *2*, 159.
(43) Yoshimura, Y. *Chem. Phys. Lett.* **2001**, *349*, 51.
(44) Kanno, H.; Tomikawa, K.; Mishima, O. *Chem. Phys. Lett.* **1998**, *293*, 412.
(45) Franks, H. S.; Evans, M. W. *J. Chem. Phys.* **1945**, *13*, 507.
(46) Braibanti, A.; Fisicaro, E.; Compari, C. *J. Therm. Anal. Calorim.* **2000**, *61*, 461.
(47) Hédoux, A.; Guinet, Y.; Capet, F.; Paccou, L.; Descamps, M. *Phys. Rev. B* **2008**, *77*, 094205.
(48) Hédoux, A.; Guinet, Y.; Derollez, P.; Willart, J. F.; Capet, F.; Descamps, M. *J Phys: Condens. Matter* **2003**, *15*, 8647.
(49) Panick, G.; Malessa, R.; Winter, R.; Rapp, G.; Frye, K. J.; Royer, C. A. *J. Mol. Biol.* **1998**, *275*, 389.
(50) Peng, X.; Jonas, J.; Silva, J. L. *Proc. Natl. Acad. Sci. U.S.A.* **1993**, *90*, 1776.
(51) Schroer, M.; Paulus, M.; Jeworrek, C.; Krywka, C.; Schmacke, S.; Zhai, Y.; Wieland, F.; Sahle, C.; Chimenti, M.; Royer, C. A.; Garcia-Moreno, B.; Tolan, M.; Winter, R. *Biophys. J.* **2010**, *99*, 3430.
(52) Ando, N.; Barstow, B.; Baase, W.; Fields, A.; Matthews, B.; Gruner, S. *Biochemistry* **2008**, *47*, 11097.
(53) Panick, G.; Malessa, R.; Winter, R. *Biochemistry* **1999**, *38*, 6512.
(54) Li, T. M.; Hook, J. W.; Drickamer, H. G.; Weber, G. *Biochemistry* **1976**, *15*, 5571.
(55) Royer, C. A. *Biochim. Biophys. Acta* **2002**, *1595*, 201.
(56) Zip, A.; Kauzmann, W. *Biochemistry* **1973**, *12*, 4217.
(57) Carter, J. V.; Knox, D. G.; Rosenberg, A. *J. Biol. Chem.* **1978**, *253*, 1947.
(58) Dadarlat, V. M.; Post, C. B. *Biophys. J.* **2006**, *91*, 4544.
(59) Marques, M. I.; Borreguero, J. M.; Stanley, H. E.; Dokholyan, N. V. *Phys. Rev. Lett.* **2003**, *91*, 138103.

(60) Efimova, Y. M.; Haemers, S.; Wierczinski, B.; Norde, W.; van-Well, A. A. *Biopolymers* **2007**, *85*, 264.
(61) Cioni, P.; Strambini, G. B. *Biophys. J.* **2002**, *82*, 3246.
(62) Makhatadze, G. I.; Glore, G. M.; Gronenborn, A. M. *Nat. Struct. Biol.* **1995**, *2*, 852.
(63) Diehl, M.; Doster, W.; Petry, W.; Schober, H. *Biophys. J.* **1997**, *73*, 2726.
(64) Dellerue, S.; Bellissent-Funel, M.-C. *Chem. Phys.* **2000**, *258*, 315.
(65) Sarupria, S.; Garde, S. *Phys. Rev. Lett.* **2009**, *103*, 037803.
(66) Ngarize, S.; Herman, H.; Adams, A.; Howell, N. *J. Agric. Food Chem.* **2004**, *52*, 6470.